

Growth rates of the electrostatic waves in the upper-hybrid band

J. Benáček¹ and M. Karlický²

¹ Department of Theoretical Physics and Astrophysics, Masaryk University, Kotlářská 2, CZ – 611 37 Brno, Czech Republic

² Astronomical Institute of the Czech Academy of Sciences, Fričova 298, CZ – 251 65 Ondřejov, Czech Republic

Received ; accepted

ABSTRACT

Context. The electrostatic waves with the frequencies close to the upper-hybrid frequency (the upper-hybrid band) are important for the generation of solar radio zebras.

Aims. Considering the plasma composed from the thermal background plasma and hot and rare plasma component in the form of the Dory-Guest-Harris distribution, we study the growth rates of the electrostatic waves in the upper-hybrid band.

Methods. We use both analytical and numerical methods.

Results. Varying the ratio of the electron-plasma and electron-cyclotron frequencies ω_{pe}/ω_{ce} in the range of 4.0-5.3 and using analytical expressions we compute the growth rates γ and dispersion branches of the electrostatic waves in the $\omega - k_{\perp}$ domain. In real plasma, the instabilities of waves with different dispersion branches can start simultaneously; therefore we define and compute the integrated growth rate Γ . For maximal and minimal Γ we show locations of the growth rates γ and dispersion branches in the $\omega - k_{\perp}$ domain. We find that Γ has a maximum when the dispersion branches not only cross the region with high growth rates γ but when the dispersion branches in this region are sufficiently long and wide. Around the value of $\omega_{pe}/\omega_{ce} = 4.95$, we recognize an exciting interchange of dispersion branches, where it is difficult to distinguish types of waves. We also analyze the effects of changes in the background plasma and hot component temperatures. Then in the same range of ω_{pe}/ω_{ce} we compute the growth rate of the electrostatic waves (which is naturally the integrated growth rate Γ) using a 3-dimensional Particle-in-Cell model. Finally, we compare both analytical and numerical results.

Key words. Instabilities – Methods: analytical – Methods: numerical – Sun: radio radiation

1. Introduction

Solar radio zebras belong to the most interesting fine structures used in diagnostics of solar flare plasmas. Among many models of these zebras, the model based on the double plasma resonance (DPR) instability belongs to the most popular (Zhelezniakov & Zlotnik 1975b; Melrose & Dulk 1982; Zaitsev & Stepanov 1983; Winglee & Dulk 1986; Ledenev et al. 2001; Zlotnik 2013; Karlický & Yasnov 2015, 2018b,a).

This instability generates the upper-hybrid waves with the frequency

$$\omega_{UH}^2 = \omega_{pe}^2 + \omega_{ce}^2 + 3k_{\perp}^2 v_{tb}^2, \quad (1)$$

when the resonance condition

$$\omega - \frac{k_{\parallel} u_{\parallel}}{\gamma_{rel}} - \frac{s\omega_{ce}}{\gamma_{rel}} = 0, \quad (2)$$

is fulfilled. Here ω , ω_{pe} , and ω_{ce} are the wave, electron-plasma, and electron-cyclotron frequency, $\mathbf{k} = (k_{\parallel}, k_{\perp})$ is wave vector, v_{tb} the thermal electron velocity of the background plasma, $\mathbf{u} = (u_{\perp}, u_{\parallel})$, $u_{\perp} = p_{\perp}/m_e$, and

$u_{\parallel} = p_{\parallel}/m_e$ are the hot electron velocities perpendicular and parallel to the magnetic field; m_e is the electron mass, γ_{rel} is the relativistic Lorentz factor, s is the gyroharmonic number, and c is the speed of light. For details, see e.g. Benáček & Karlický (2018).

In theoretical models of the double plasma resonance instability, a two-component plasma with the background plasma having the Maxwellian distribution and hot and rare component with the Dory-Guest-Harris electron distribution for $j = 1$ (Dory et al. 1965)

$$f_{hot}(u_{\parallel}, u_{\perp}) = \frac{u_{\perp}^2}{2(2\pi)^{3/2} v_t^5} \exp\left(-\frac{u_{\perp}^2 + u_{\parallel}^2}{2v_t^2}\right), \quad (3)$$

is assumed. Here v_t we call the thermal velocity of hot electrons, although the distribution function in this relation is not Maxwellian.

Besides the zebra model based on DPR instability, there is the model that explains zebras by nonlinear interaction of Bernstein modes (Kuznetsov 2005). In principle, Bernstein modes can also be generated in the upper-hybrid band. Both the upper-hybrid waves and Bernstein mode are the electrostatic (longitudinal) waves. Because in the upper-hybrid band in some cases it is difficult to distinguish these

Send offprint requests to: , e-mail: jbenacek@physics.muni.cz

waves therefore in the following we use the general term - the electrostatic waves.

The primary purpose of the present study is an analysis of the growth rates of the electrostatic waves in relation to positions of dispersion branches in the upper-hybrid band. We make this analysis analytically and then for comparison numerically using the 3-dimensional Particle-in-Cell (PIC) model.

The paper is structured as follows. In Section 2 we start with a theory of the electrostatic (longitudinal) waves perpendicular to the magnetic field. The growth rates of these waves in the upper-hybrid band derived analytically are in Section 3. In Section 4 there are the growth rates obtained numerically. Discussion of the results and conclusions are in Sections 5.

2. Basic relations for the electrostatic waves in a two-component plasma

Let us consider the plasma composed from the background Maxwellian plasma with the density n_e and the thermal velocity v_{tb} and hot plasma having the density n_h and the "thermal" velocity v_t , where $n_h \ll n_e$. Then the dispersion relation of the electrostatic (longitudinal) waves in such a plasma is given by the permittivity tensor

$$\epsilon_{\parallel} = \epsilon_{\parallel}^{(0)} + \epsilon_{\parallel}^{(1)} = 0, \quad (4)$$

where the term $\epsilon_{\parallel}^{(0)}$ corresponds to the background Maxwellian plasma and the term $\epsilon_{\parallel}^{(1)}$ is a correction to the hot and rare plasma component.

In our case with $n_h \ll n_e$ and in agreement with Chen (1974); Zhelezniakov (1997); Fitzpatrick (2015) we can write

$$\epsilon_{\parallel}^{(0)} = 1 - 2\omega_{pe}^2 \frac{e^{-\lambda}}{\lambda} \sum_{l=1}^{\infty} \frac{l^2 I_l(\lambda)}{\omega^2 - l^2 \omega_{ce}^2} = 0, \quad (5)$$

$$\omega_{pe}^2 = \frac{n_e e^2}{m_e \epsilon_0}, \quad \lambda = \frac{k_{\perp}^2 v_{tb}^2}{\omega_{ce}^2}, \quad (6)$$

where ω_{pe} and ω_{ce} is the plasma frequency of the background plasma and the electron cyclotron frequency, λ is the dimensionless parameter, $I_l(\lambda)$ is the modified Bessel function of l th order, $Z(\zeta_l)$ is the plasma dispersion function, m_e is the electron mass, e is the electron charge, ω is the wave frequency, $\mathbf{k} = (k_{\parallel}, k_{\perp})$ is the wave vector parallel and perpendicular to the direction of the magnetic field respectively.

Solutions of the real part of Equation 5 are the dispersion relations for the upper-hybrid waves as well as for the Bernstein waves. Because in the present paper we are interested about these waves in the upper-hybrid band, where sometimes is a problem to distinguish between these waves, therefore in the following we use for them the common term: the electrostatic waves.

For the growth rate of these waves, we can write (Zhelezniakov & Zlotnik 1975a)

$$\gamma(\omega, k_{\perp}) = - \frac{\text{Im} \epsilon_{\parallel}^{(1)}}{\left[\frac{\partial \text{Re} \epsilon_{\parallel}^{(0)}}{\partial \omega} \right]_{\epsilon_{\parallel}^{(0)}=0}}. \quad (7)$$

In accordance with Kuznetsov (2005, Appendix A) the nominator of Equation 7 can be written as

$$\text{Im}(\epsilon_{\parallel}^{(1)}) = -2\pi^2 m_e^4 a b^2 \frac{\omega_{pe}^2}{k^2} \sum_{l=1}^{\infty} \int_0^{\phi_{\max}} \left[J_l \left(\frac{\gamma_{\text{rel}} k_{\perp} v_{\perp}}{\omega_{ce}} \right) \times \frac{\gamma_{\text{rel}}^5 \sin \phi}{\frac{\partial \psi}{\partial \rho}} \left(k_{\parallel} \frac{\partial f}{\partial p_{\parallel}} + \frac{l \omega_{ce}}{\gamma_{\text{rel}} v_{\perp}} \frac{\partial f}{\partial p_{\perp}} \right) \right] d\phi, \quad (8)$$

$$\frac{\partial \psi}{\partial \rho} = \frac{\gamma_{\text{rel}}^2 l \omega_{ce}}{c^2} (v_{\parallel} (v_{\parallel} - v_0) + v_{\perp}^2) - \gamma_{\text{rel}} k_{\parallel} (v_{\parallel} - v_0), \quad (9)$$

$$\psi_{\max} = \left\{ \begin{array}{ll} \pi, & k_{\parallel}^2 c^2 \leq \omega^2, \\ \arccos \left(\frac{k_{\parallel} v_0 - \omega}{k_{\parallel} a} \right) & k_{\parallel}^2 c^2 > \omega^2, \end{array} \right\}, \quad (10)$$

$$v_{\parallel} = v_0 - a \cos(\phi), \quad v_{\perp} = b \sin(\phi), \quad (11)$$

where

$$v_0 = \frac{\omega k_{\parallel} c^2}{k_{\parallel}^2 c^2 + l^2 \omega_{ce}^2}, \quad (12)$$

$$a^2 = \frac{l^2 \omega_{ce}^2 c^2 (k_{\parallel}^2 c^2 + l^2 \omega_{ce}^2 - \omega^2)}{(k_{\parallel}^2 c^2 + l^2 \omega_{ce}^2)^2}, \quad (13)$$

$$b^2 = \frac{c^2 (k_{\parallel}^2 c^2 + l^2 \omega_{ce}^2 - \omega^2)}{k_{\parallel}^2 c^2 + l^2 \omega_{ce}^2}, \quad (14)$$

where c is the speed of light, v_{\parallel} and v_{\perp} are the velocities on resonance ellipse in Equation 2 and f is the electron velocity distribution function in the form

$$f(v_{\perp}, v_{\parallel}) = f_0(v_{\perp}, v_{\parallel}) + \frac{n_h}{n_e} f_{\text{hot}}(v_{\perp}, v_{\parallel}). \quad (15)$$

The f_0 means the background Maxwellian distribution for temperature v_{tb} , f_{hot} is in our case the Dory-Guest-Harris distribution given by Equation 3 described by the "thermal" velocity v_t and $J_l(\lambda)$ is the Bessel function.

Furthermore, the denominator of Equation 7 can be expressed as

$$\frac{\partial \epsilon_{\parallel}}{\partial \omega} = 4\omega \omega_{pe}^2 \frac{e^{-\lambda}}{\lambda} \sum_{l=1}^{\infty} \frac{l^2 I_l(\lambda)}{(\omega^2 - l^2 \omega_{ce}^2)^2}. \quad (16)$$

3. Analytical growth rates

In this Section, we compute the growth rates using analytically derived equations expressed in the previous Section. As an example we make computations for the ratio of the electron-plasma and electron-cyclotron frequency (ω_{pe}/ω_{ce}) in the 4.0-5.3 range. Namely, we want to determine the growth rates also for a non-integer ratio of ω_{pe}/ω_{ce} . The relatively low values of this ratio are chosen due to a comparison with the numerical simulations, where computations with the low values of ω_{pe}/ω_{ce} are more reliable.

If we do not mention explicitly, in our analytical computations and also in the following numerical simulations, we use the parameters shown in Table 1. Considering the

Parameter	Value
v_{tb}	0.018 c (2 MK)
v_t	0.2 c
n_e	10^{11} cm^{-3}
n_e/n_h	32
f_{hot}	DGH
ω_{pe}	$2\pi \times 2.85 \times 10^9 \text{ s}^{-1}$
$k_{\perp}c/\omega_{pe}$	0 – 15 range
ω/ω_{pe}	0 – 2 range

Table 1: Parameters used for computing of the growth rates.

propagation of waves in the strictly perpendicular direction to the magnetic field ($k_{\parallel} = 0$) and using Equations 5 we compute their dispersion branches and growth rates in the $\omega - k_{\perp}$ domain. In summation we use $\sum_{l=-40}^{40}$ instead of $\sum_{l=-\infty}^{\infty}$.

Roots of Equation 5 (dispersion branches) are searched using the least-square method from SciPy package in the Python. From this method, we also get the covariance parameter $\sigma^2(\omega, k_{\perp})$ which can be interpreted as the "relative width" of the dispersion branch.

Because we want to compare the results obtained from analytical relations with those from the following PIC simulations, where the growth rate is given by compositions of growth rates in the whole $\omega - k_{\perp}$ domain, we need to integrate the analytical growth rates in this $\omega - k_{\perp}$ domain.

The integrated growth rate Γ can be expressed as

$$\Gamma = \frac{1}{\Gamma_0} \int \gamma(\omega, k_{\perp}) \sigma(\omega, k_{\perp}) \delta(\epsilon_{\parallel}^{(0)}(\omega, k_{\perp})) d\omega dk_{\perp}, \quad (17)$$

where δ is the Dirac delta function and $\gamma(\omega, k_{\perp})$ is the growth rate at the specific ω and k_{\perp} . This integral counts the growth rates over the dispersion branches of the electrostatic waves with their weight σ . The function Γ_0 is the normalization factor

$$\Gamma_0 = \int \sigma(\omega, k_{\perp}) \delta(\epsilon_{\parallel}^{(0)}(\omega, k_{\perp})) d\omega dk_{\perp}. \quad (18)$$

In our case the integral is computed over the $\omega - k_{\perp}$ area with $\omega/\omega_{pe} \in (0, 2)$ and $k_{\perp}c/\omega_{pe} \in (0, 20)$. At higher frequencies the branches are very narrow and thus do not contribute effectively to the integrated growth rate and at higher values of the wave vectors $\gamma = 0$.

Using the plasma parameters from Table 1 we computed the integrated growth rates Γ (Equation 17) for the ratios $\omega_{pe}/\omega_{ce} = 4.0 - 5.3$, see Figure 1. As can be seen in this figure, the maximum of Γ is for $\omega_{pe}/\omega_{ce} = 4.8$ and the minimum for $\omega_{pe}/\omega_{ce} = 4.4$.

Now, a question arises how the integrated growth rate Γ is related to the positions of the growth rates γ and dispersion branches in the $\omega - k_{\perp}$ domain. To answer this question, we compute the growth rates γ and dispersion branches in the $\omega - k_{\perp}$ domain for the maximal and minimal values of the integrated growth rate Γ . The results are shown in Figure 2, where the growth rates and dispersion branches in a broad area of (ω, k_{\perp}) (Plots a, b) and detailed views in the upper-hybrid band (Plots c, d) are presented. We note that the parts of dispersion branches with the "width" σ less than 10^{-6} are very narrow and thus they are not represented in the figure, see also the following and Table 2.

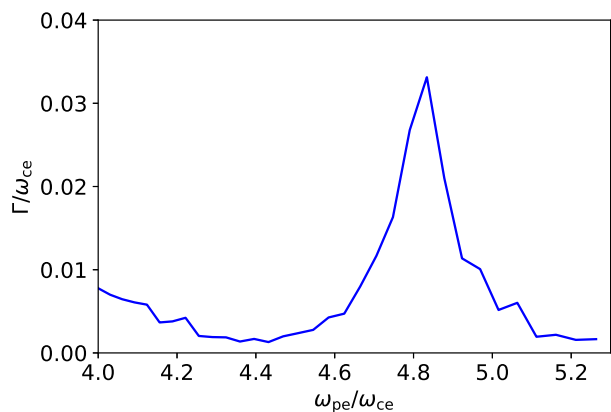


Fig. 1: Integrated growth rate Γ computed from Equation 17 as a function of the ratio ω_{pe}/ω_{ce} normalized to ω_{ce} for the parameters given in Table 1. Its maximum is for $\omega_{pe}/\omega_{ce} = 4.8$ and minimum for $\omega_{pe}/\omega_{ce} = 4.4$.

Maximum		Minimum	
$\omega_{pe}/\omega_{ce} = 4.8$		$\omega_{pe}/\omega_{ce} = 4.4$	
ω_{branch}	σ	ω_{branch}	σ
0.335	7.4×10^{-3}	0.374	9.1×10^{-3}
0.593	1.0×10^{-2}	0.652	1.2×10^{-2}
0.821	1.2×10^{-2}	0.897	2.0×10^{-2}
1.029	9.9×10^{-2}	1.068	4.0×10^{-1}
1.073	3.4×10^{-1}	1.138	2.2×10^{-2}
1.248	6.6×10^{-4}	1.362	1.46×10^{-4}
1.456	1.5×10^{-5}	1.589	3.95×10^{-6}

Table 2: Relative width of the dispersion branches σ for the maximum Γ with $\omega_{pe}/\omega_{ce} = 4.8$ (see Figure 1) and for the minimal Γ with $\omega_{pe}/\omega_{ce} = 4.4$. ω_{branch} means the frequency of the dispersion branch for $k_{\perp}c/\omega_{pe} = 10$.

As seen here, in the $\omega - k_{\perp}$ domain there are the regions with the high growth rates. The maximal growth rate in the field of view of Figure 2c is $\gamma/\omega_{ce} = 0.073$. Comparing the cases with the maximal and minimal integrated growth rates Γ , we can see differences in distributions of the dispersion branches and growth rate regions. While in the case with the maximal Γ the dispersion branches in most cases cross the region with the high growth rates, in the case with the minimal Γ the thickest branches are out these regions. Note that for the integrated growth rate is important not only this crossing over these regions but also the lengths and width (area) of the dispersion branches over these regions. Namely, the wave energy is given by the wave energy density in the area unit times the area. We suppose that the width of the dispersion branch is proportional to σ calculated during computations of the dispersion branches. Thus, there are the dispersion branches, which go through the high growth rate regions even for the minimal growth rate Γ (see Figure 2b, e.g. the region $\omega/\omega_{pe} = 1.4$, $k = 6 - 15$), but their width is very small and therefore do not significantly influence the integrated growth rate Γ .

In the Table 2 we present the relative width of different dispersion branches σ . A difference in the relative width can be several orders. The maximal Γ appears, when the dispersion branch with the highest relative width crosses the high growth rate area around the plasma frequency, see

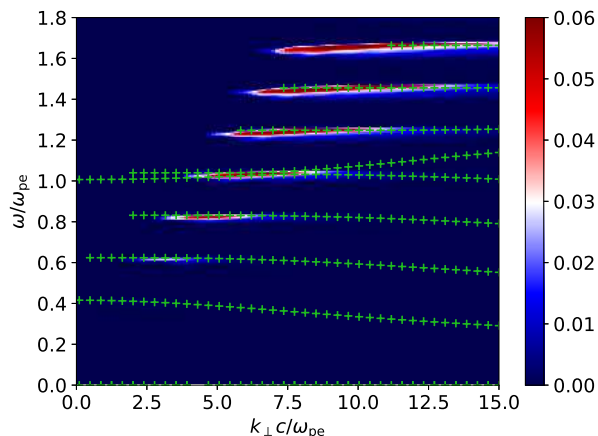
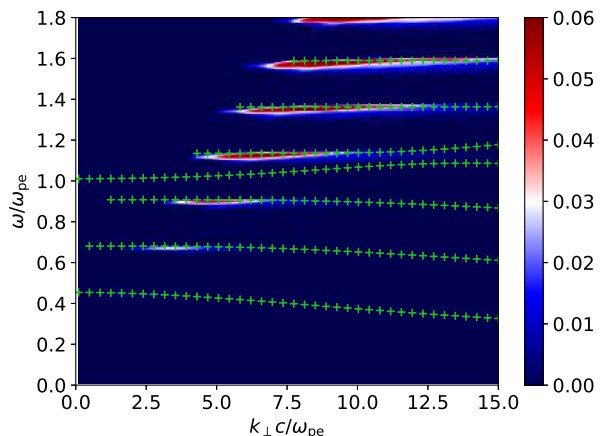
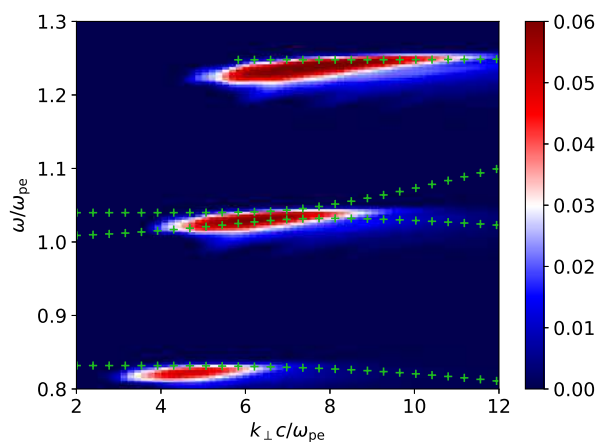
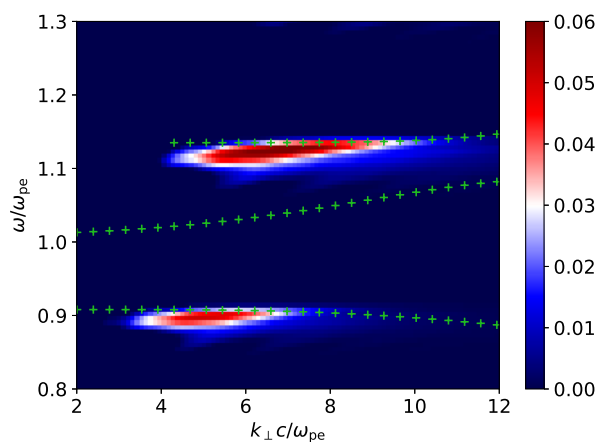

(a) Growth rates and dispersion branches for $\omega_{pe}/\omega_{ce} = 4.8$.

(b) Growth rates and dispersion branches for $\omega_{pe}/\omega_{ce} = 4.4$.

(c) Detailed view for $\omega_{pe}/\omega_{ce} = 4.8$.

(d) Detailed view for $\omega_{pe}/\omega_{ce} = 4.4$.

Fig. 2: Analytical growth rates γ/ω_{ce} in the $\omega - k_{\perp}$ domain (the blue-red scale) for the maximal value of Γ , i.e., for $\omega_{pe}/\omega_{ce} = 4.8$ and for the minimal value of Γ , i.e., for $\omega_{pe}/\omega_{ce} = 4.4$ taken from Figure 1. The green crosses show dispersion branches of the electrostatic waves. *Plots a, b*: The growth rates in a broad range of (ω, k_{\perp}) . *Plots c, d*: Detailed view on the growth rates and dispersion branches in the upper-hybrid band.

Figure 2c. It is interesting that in this case, two dispersion branches of the electrostatic waves are very close to each other.

To show how the dispersion branches are crossing and interconnecting, in Figure 3 we present the dispersion branches superimposed on the growth rates γ for three values of the ratio $\omega_{pe}/\omega_{ce} = 4.925, 4.950$ and 4.975 . Here in the left part of the figure we can see that the dispersion branch, which is firstly under the plasma frequency, is going up to higher frequencies with decreasing ω_{pe}/ω_{ce} . During this shift it extrudes the upper dispersion branch up (Figure 3c). In the region where the branches meet a knee on the bottom dispersion branch is formed; i.e., for lower k_{\perp} than this knee there is a part of the dispersion branch with the normal dispersion and for higher k_{\perp} is the part with the anomalous dispersion (Figure 3c). Thus, in some cases, the electrostatic waves are generated at the part with the

normal dispersion and in others at that with the anomalous dispersion.

For the value of $v_{tb} = 0.018 c$ considered in Figure 3a,c,e, this interplay of dispersion branches happens slightly out of the region with high growth rates; therefore the integrated growth rate Γ has not the maximal value. However, we found that for lower background thermal velocity ($v_{tb} = 0.007 c$), the dispersion branches not only meet, but they also are in the region with high growth rates (Figure 3d) and thus for these plasma parameters the high integrated growth rate Γ can be expected.

We also studied the distribution of the growth rates γ and dispersion branches in dependence on the background plasma temperature (Figure 4). With increasing the background plasma temperature the center of the region with the high growth rates remains at the same position, but the size of this region decreases. Moreover, the point, where dispersion branches meet and cross the region with the high

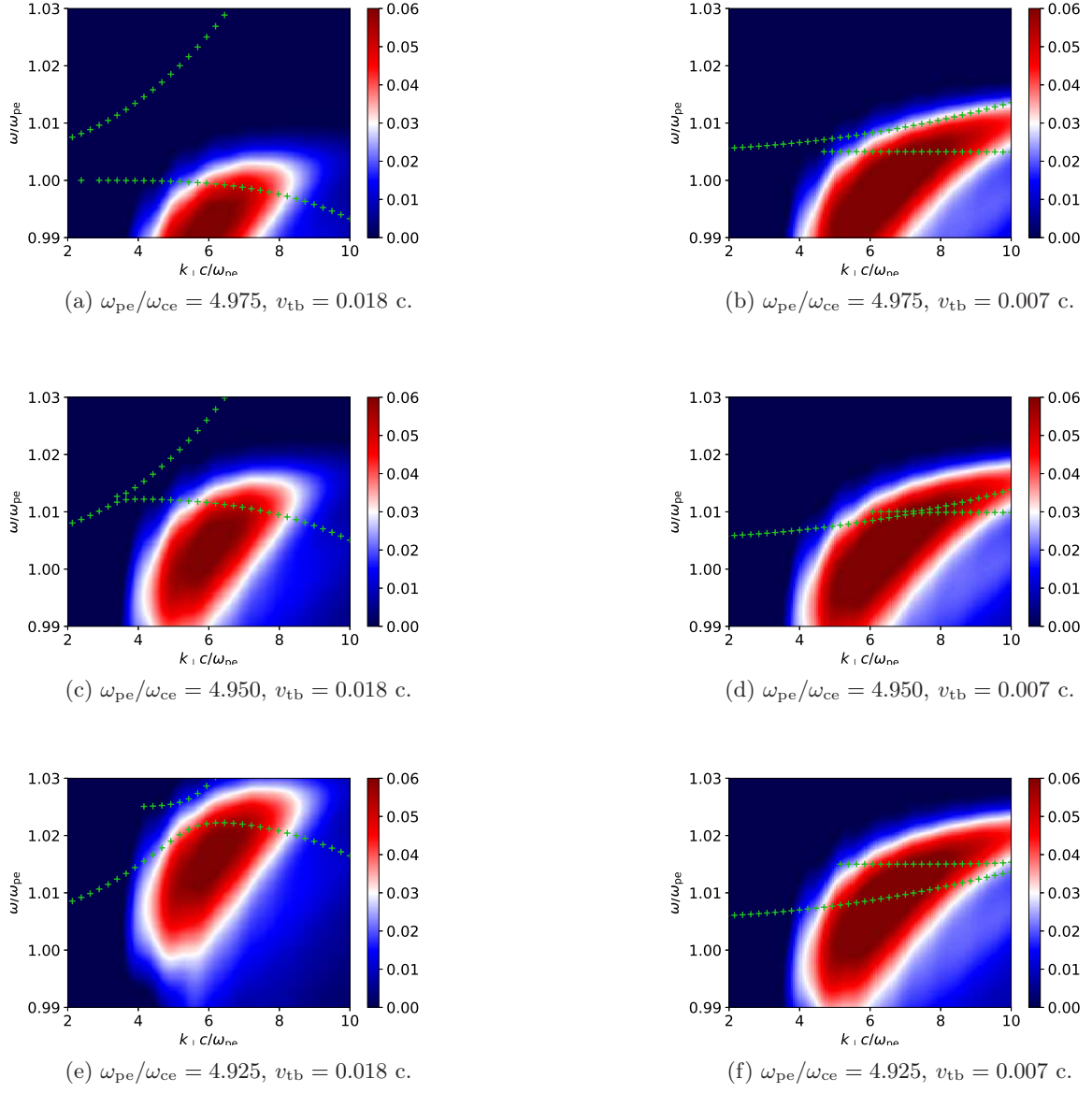


Fig. 3: Analytical growth rates normalized to ω_{ce} and dispersion branches in dependence on ratio $\omega_{pe}/\omega_{ce} \in (4.925, 4.950, 4.975)$ for two background temperatures: $v_{tb} = 0.018$ c (a, c, e) and $v_{tb} = 0.007$ c (b, d, f).

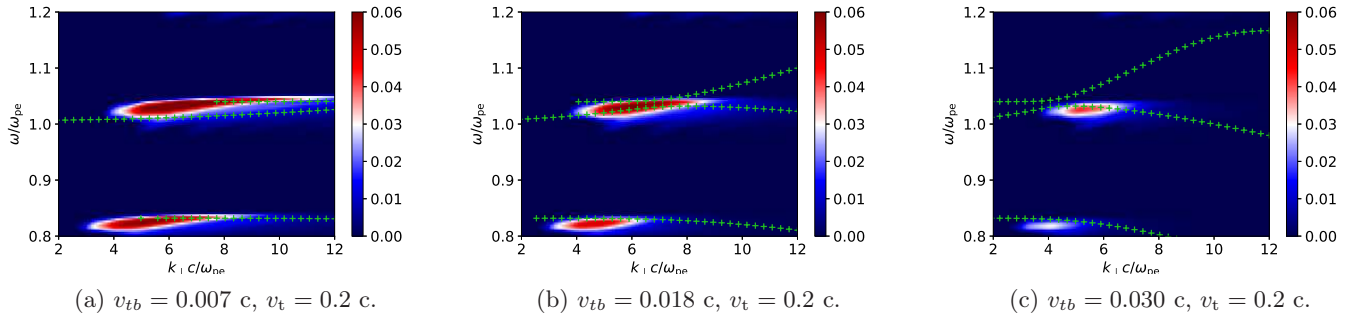


Fig. 4: Analytical growth rates normalized to ω_{ce} (blue-red scale) and dispersion branches in dependence on the background thermal velocity v_{tb} . The thermal velocity of the hot component $v_t = 0.2$ c and $\omega_{pe}/\omega_{ce} = 4.8$ are kept constant in all these cases.

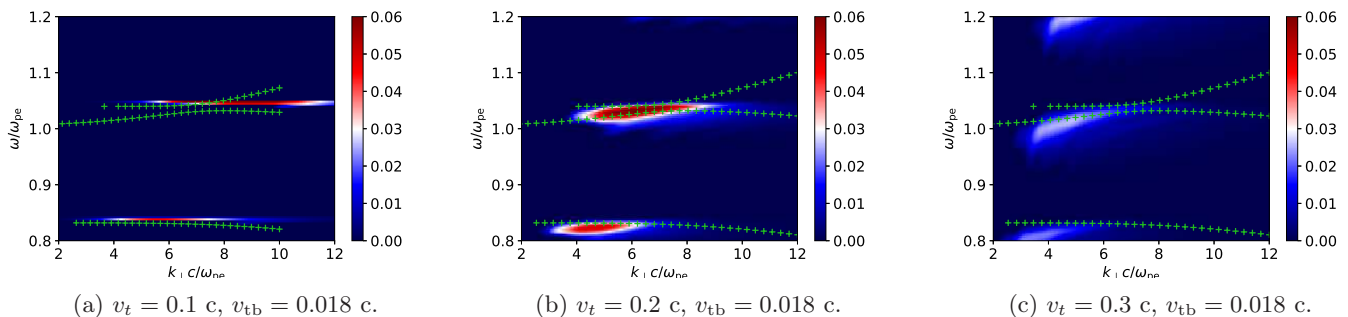


Fig. 5: Analytical growth rates normalized to ω_{ce} and dispersion branches in dependence on the hot electrons velocity v_t , $v_{tb} = 0.018 c$ and $\omega_{pe}/\omega_{ce} = 4.8$ are kept constant.

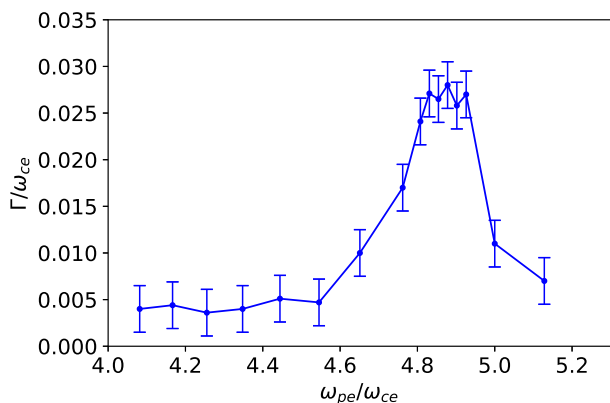


Fig. 6: Growth rates from PIC simulations as a function of the ratio ω_{pe}/ω_{ce} for $v_t = 0.2 c$, $v_{tb} = 0.018 c$. Compare it with Γ in Figure 1.

growth rates, shifts to lower k_{\perp} . The reason is that for the constant $\lambda = k_{\perp}^2 v_{tb}^2 / \omega_{ce}^2$ the component of the wave vector k_{\perp} has to decrease when v_{tb} increases. It implies that for the dispersion branches close to the plasma frequency and $v_{tb} < 0.007 c$ the electrostatic waves are generated at the normal part of the dispersion branch, while for higher thermal velocities in its anomalous part.

On the other hand, Figure 5 shows the distribution of the growth rates and dispersion branches in dependence on the "thermal" velocity of hot electrons v_t . With increasing this velocity the position of the region with high growth rates shifts to lower k_{\perp} . For a constant argument in the Bessel function in Equation 8, $\text{const} = \Gamma v_{\perp} k_{\perp} / \omega_{ce}$, k_{\perp} decreases as v_{\perp} increases. The region with high growth rates expands along the frequency axis with increasing v_t . However, the maximal values of γ in the region center decrease. The reason is that the value of the term $\partial f(v_{\perp}, v_{\parallel}) / \partial v_{\perp}$ decreases with increasing of v_t . For temperatures $v_t < 0.15 c$ the area of the region with high growth rates γ is so narrow that the integrated growth rate Γ is negligible.

4. Numerical growth rates

We make simulations using a 3D Particle-in-Cell (PIC) relativistic model (Buneman & Storey 1985; Matsumoto & Omura 1993; Karlický & Bárta 2008;

Benáček & Karlický 2018) with multi-core Message Passing Interface (MPI) parallelization. Further details can be found in Matsumoto & Omura (1993, p.67-84) and on the link below.¹

The model size is $48\Delta \times 48\Delta \times 16\Delta$ in x, y, z -directions respectively. The generated electrostatic waves are in $x - y$ plane, z coordinate corresponds to the magnetic field direction. One run takes 80 000 time steps with the time step $\omega_{pe} t = 0.025$. The electron distribution function is DGH distribution, the number of electrons per cell is $n_e = 960$, the ratio of densities of the background plasma and hot electrons is $n_e/n_h = 32$, $\omega_{pe}/\omega_{ce} = 4-5.3$. Other parameters are as in Table 1.

Varying the ratio of ω_{pe}/ω_{ce} in the range 4.0-5.3 we made the PIC simulations and estimated the growth rates from the growth of the electrostatic wave energy (Figure 6). Note that these growth rates correspond to the integrated growth rates Γ in the analytical approach. The profile of the growth rate and the growth rate values are very similar to that presented in Figure 1. In the range of $\omega_{pe}/\omega_{ce} = 4.1-4.5$ the growth rate is very weak, and at $\omega_{pe}/\omega_{ce} = 4.88$ there is the growth rate maximum. It is at slightly higher values of ω_{pe}/ω_{ce} comparing with the maximum Γ shown in Figure 1.

5. Discussion and conclusions

In this paper we computed two types of the growth rate: a) the growth rate γ that corresponds to one point in the $\omega - k_{\perp}$ domain, i.e., located at one specific dispersion branch and b) the growth rate Γ integrated over the upper-hybrid band, where we took into account the fact that in real conditions as well as in PIC simulations the instability can start simultaneously not only at one point in the $\omega - k_{\perp}$ domain, but in some area in this domain and even on several dispersion branches. While the maximal growth rate γ/ω_{ce} is found as 0.073, the integrated growth rate Γ/ω_{ce} is about 0.03. The maximal growth rate γ agrees to those presented by Zhelezniakov & Zlotnik (1975a); Winglee & Dulk (1986); Benáček et al. (2017), but due to various thermal velocities, plasma densities and magnetic fields used in these papers this comparison is not straightforward. We also compared the maximal Γ from the present PIC simulations with that in our previous paper (Benáček & Karlický

¹ <https://www.terrapub.co.jp/e-library/cspp/text/10.txt>.

2018). We found that due to an error in the growth-rate normalization in our previous paper the growth rate in this paper was overestimated 20 times. Considering this correction the maximal growth rate Γ from the present paper agrees to that in the paper by Benáček & Karlický (2018).

We found that the profile of the integrated growth rate Γ obtained by analytical calculations and that in PIC simulations are very similar and their maxima are at almost the same value of ω_{pe}/ω_{ce} . This difference can be explained by slightly different positions of dispersion branches in the analytical and numerical approaches. Namely, the condition $n_h \ll n_e$ which is used in the analytical approach, in PIC simulations is difficult to fulfill, which has an impact on positions of dispersion branches in PIC model. We found that the growth rate peak in PIC simulations is broader than that in the analytical approach. We think that it is because in the PIC model there can also be the electrostatic waves with $k_{\parallel} \neq 0$.

In dispersion diagrams with dispersion branches and growth rate regions, calculated analytically, we showed how the plasma parameters influence their mutual positions in the $\omega - k_{\perp}$ domain. We found that when a sufficiently "wide" dispersion branch crosses the region with high growth rates along with a sufficient length then the integrated growth rate Γ is high.

Varying the plasma parameters, we showed that in some range of ω_{pe}/ω_{ce} the dispersion branches can meet and change the form to that with a knee. We found that sometimes a dominant contribution to the integrated growth rate Γ comes from the normal part of the dispersion branch and sometimes from the anomalous part. Moreover, when some branches meet then it is sometimes difficult to distinguish a type of the electrostatic wave.

We described details of how the integrated growth rate Γ is influenced by the temperature of the background plasma and "thermal" velocity of the hot component. The background temperature has a low impact on the position of the growth rate region. The velocity of the hot component changes the growth rate more dramatically. Decreasing this velocity the region is shrinking. Below the temperatures $v_t < 0.15 c$ we found no significant or very narrow growth rate peak. This is in agreement with PIC simulations made by Benáček & Karlický (2018).

We found that in the upper-hybrid band there can be several dispersion branches of the electrostatic waves perpendicular to the magnetic field with normal and anomalous dispersions. We showed that sometimes two branches can even cross the same growth-rate region in the $\omega - k_{\perp}$ domain. In the double plasma resonance (DPR) models of solar radio zebras only the instability of the upper-hybrid waves with the normal dispersion (Eq. 1) is considered. Thus, in new models of zebras, based on DPR instability, instabilities on all branches in the upper-hybrid band should be taken into account.

Acknowledgements. We acknowledge support from Grants 17-16447S, 18-09072S and 19-09489S of the Grant Agency of the Czech Republic. This work was supported by The Ministry of Education, Youth and Sports from the Large Infrastructures for Research, Experimental Development and Innovations project „IT4Innovations National Supercomputing Center – LM2015070“.

References

Benáček, J. & Karlický, M. 2018, A&A, 611, A60

- Benáček, J., Karlický, M., & Yasnov, L. 2017, A&A, 555, A1
 Buneman, O. & Storey, L. R. O. 1985, Simulations of fusion plasmas by A 3-D, E-M particle code, Tech. rep.
 Chen, F. F. 1974, Introduction to plasma physics
 Dory, R. A., Guest, G. E., & Harris, E. G. 1965, Physical Review Letters, 14, 131
 Fitzpatrick, R. 2015, Plasma physics: an introduction (CRC Press)
 Karlický, M. & Bárta, M. 2008, Sol. Phys., 247, 335
 Karlický, M. & Yasnov, L. V. 2015, A&A, 581, A115
 Karlický, M. & Yasnov, L. V. 2018a, ApJ, 867, 28
 Karlický, M. & Yasnov, L. V. 2018b, A&A, 618, A60
 Kuznetsov, A. A. 2005, A&A, 438, 341
 Ledenev, V. G., Karlický, M., Yan, Y., & Fu, Q. 2001, Sol. Phys., 202, 71
 Matsumoto, H. & Omura, Y. 1993, Computer space plasma physics: simulation techniques and software, Terra Scientific Pub. Co, p.305
 Melrose, D. B. & Dulk, G. A. 1982, ApJ, 259, 844
 Winglee, R. M. & Dulk, G. A. 1986, ApJ, 307, 808
 Zaitsev, V. V. & Stepanov, A. V. 1983, Sol. Phys., 88, 297
 Zhelezniakov, V. V. 1997, Radiation in astrophysical plasmas [in Russian]; Original Russian Title — “Izlucheniye v astrofizicheskoy plazme”
 Zhelezniakov, V. V. & Zlotnik, E. I. 1975a, Sol. Phys., 43, 431
 Zhelezniakov, V. V. & Zlotnik, E. Y. 1975b, Sol. Phys., 44, 461
 Zlotnik, E. Y. 2013, Sol. Phys., 284, 579